



The Impact Analysis of Cable Rupture during Construction on the Seismic Response of a Low Tower Cable-Stayed Bridge

Jingyu Li^a, Mingbo Ding^{b*}, Jinhua Lu^c

School of Civil Engineering, Lanzhou Jiaotong University, Lanzhou, Gansu, 730070, China

^aemail: 1094827462@qq.com, ^c814926385@qq.com

^bCorresponding author's e-mail: ding_mingbo@126.com

Abstract. In order to study the seismic response of the structure during the construction of a low tower cable-stayed bridge due to cable breakage, a full bridge finite element model was established using the finite element software Midas Civil, with the BoluoDongjiang Bridge as the engineering background. Three different types of seismic wave records were input for seismic response analysis, and the influence of cable breakage at different positions on the seismic response of key parts of the low tower cable-stayed bridge was explored. The results show that cable breakage at different positions will have varying degrees of impact on the seismic response of the structure, with the outer inclined cable having a greater impact on the seismic response of the structure than the inner cable breakage; Cable breakage only has a relatively significant impact on adjacent cables, and the change rate of cable force caused by different cable breakage is approximately 5% to 20%; Different types of ground motions have different seismic responses to structures, and cable breakage can increase the seismic response of the structure.

Keywords: extradosed cable-stayed bridge; cable breakage; finite element simulation; seismic response.

1 Introduction

In recent years, as a combination system bridge between continuous beam (rigid frame) bridge and cable-stayed bridge, low pylon cable-stayed bridge has achieved rapid development at home and abroad with its good structural performance and economic indicators [1-2]. Similar to conventional cable-stayed Bridges, cable cables, as an important force transmission component of low-pail cable-stayed Bridges [3], are directly arranged outside the main beam and cable tower and are in direct contact with the air. With small size and high stress, vehicle impact, fatigue and corrosion may cause serious damage to cable cables. In addition, in some extreme cases, such as fire and earthquake, the cable is more likely to be damaged or even broken. In 1979, the cable of the Maracaibo Lake Bridge in Venezuela suddenly broke due to corrosion, causing

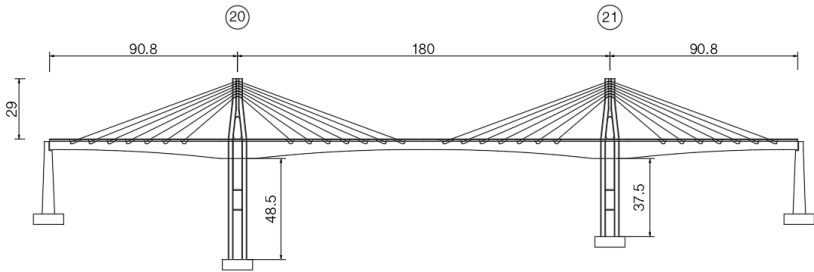
partial collapse of the bridge [4-5]. In 2001, the rust of the steel strand of the boom of Xiaonanmen Bridge in Yibin, Sichuan Province caused the partial fracture of the boom, resulting in the collapse of the main body of the bridge [6]. In 2014, a fire broke out at the top of the left column of No. 6 pier of Chishi Large Bridge under construction in Chenzhou, Hunan Province. Due to the high temperature, 9 stayed cables lost bearing capacity and broke, resulting in severe cracking of the beam [7].

Mozos[8] et al. analyzed the dynamic response of 10 cable-stayed Bridges after cable break, and studied the influence of different cable surface shapes, the instant duration of cable break and the number of cable surfaces on the dynamic response of cable-stayed Bridges. In order to study the dynamic characteristics and seismic performance of double-steel arch tower cable-stayed bridge under the action of cable damage, Huang Hua et al. [9] established a three-dimensional finite element model with finite element software Midas/Civil, and analyzed the variation rules of main beam line shape, cable force, main beam and cable tower stress under the simultaneous action of earthquake and cable breaking. By establishing a nonlinear dynamic solid finite element model, Zhang Yu et al. [7] studied the structural dynamic response of cable-stayed bridge during construction, analyzed the internal force changes of the structure, and determined the dynamic amplification factor of the structure. Khawaja Ali et al. [10] provides new insights into the comparison of cable-stayed and extradosed bridges based on the safety assessment of their stay cables. The analysis results show that cable-stayed and extradosed bridges exhibit different structural redundancies for different safety factors under the same loading conditions. Moreover, a significant increase in structural redundancy occurs with an incremental increase in the safety factors of stay cables.. Xue Xiaofeng et al. [11] established a finite element model of a cable-stayed bridge, analyzed the overall performance degradation of the cable, buckling safety factor of the main beam and stress safety factor under the condition of single cable and single pair cable damage, and determined the vulnerable position of the cable-stayed cable. Wang Yao [12] established the finite element full bridge model of the low pylon cable-stayed bridge, and studied the influence of different degree of damage of broken cables and cable cables on the natural vibration frequency and seismic response analysis results of the low pylon cable-stayed bridge. At present, most researches on cable damage of cable-stayed Bridges and low-pylon cable-stayed Bridges focus on their dynamic response and seismic response, and there are relatively few seismic researches on cable damage of low-pylon cable-stayed Bridges during construction[13-16]. It is also necessary to further study the effect of the cable damage on the remaining cable of the cable-stayed bridge in the construction stage and its effect on the seismic response of the key parts of the bridge.

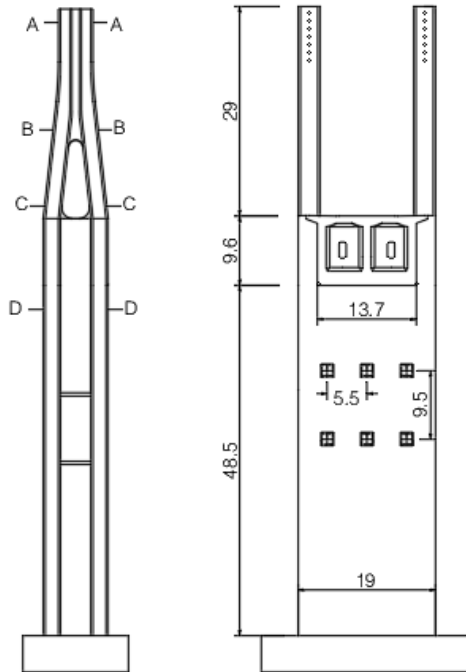
In this paper, based on the engineering background of Boluo Dongjiang Large Bridge, the influence of cable fracture on cable force under earthquake and its influence on the seismic response of key parts of low tower cable-stayed bridge is studied by establishing finite element model, which provides reference for the subsequent design and research of such Bridges.Engineering background

The Boluo Dongjiang Grand Bridge is located in Luoyang Town, Boluo County, Huizhou City. It is a double tower, four cable plane, low tower cable-stayed bridge with a tower pier beam consolidation system. The main tower adopts a double column

bridge tower form, with a tower height of 29.0m above the bridge deck and a height to span ratio of 1/6.21 above the bridge deck. The span arrangement of the main bridge is 90.8m+180m+90.8m, with a total length of 361.6m and a bridge deck width of 16.8m; To adapt to the split wire cable saddle, the tower column adopts a rectangular solid section. At the consolidation point of the tower pier beam, the bridge tower forks into two independent tower columns, forming an inverted Y shape. Each cable tower is arranged with 7 pairs of diagonal cables on both sides, arranged in a fan-shaped manner. There are a total of 28 cables in the entire bridge. The geometric structure of the bridge is shown in the Figure 1.



(a) Overall layout of the entire bridge



(b) Layout of cable tower

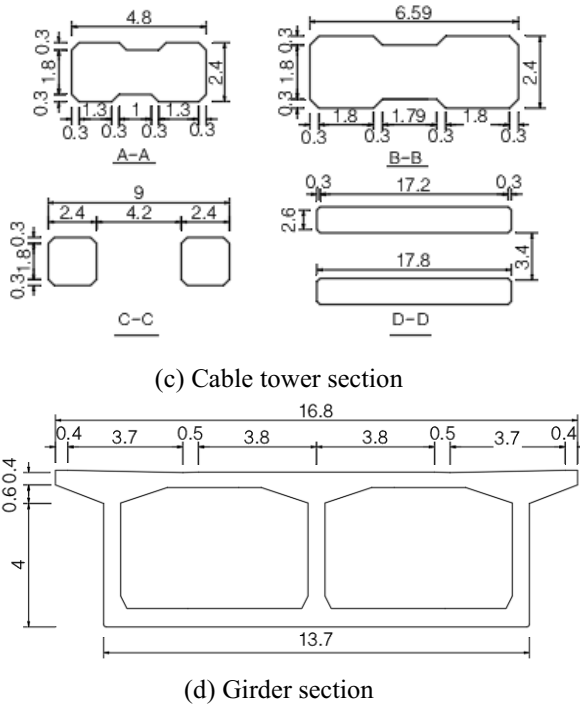


Fig. 1. Geometry of Boluodongjiang bridge(m)

2 Finite element model

A spatial finite element model of the bridge was established using Midas Civil 2020 software, consisting of 205 nodes and 196 elements. Both the main beam and cable tower were constructed using spatial beam elements. To eliminate the influence of cable sag on structural nonlinearity, a tension only truss element modified by Ernst's formula is used to simulate cable-stayed cables. Consolidation simulation is used for the boundary of the pier bottom; The rigid connection is used at the consolidation point of the tower pier beam, and the rigid connection is used between the stay cable and the main beam, and between the stay cable and the cable tower. The fracture of the stay cable is simulated using the dismantling component method[16].

The main beam and cable tower are made of C55, the bridge piers are made of C50, and the cable-stayed cables are made of epoxy coated unbonded prestressed steel strands; The main beams, cable towers, and cable numbers of the Boluo Dongjiang Grand Bridge are shown in Figure 2. Among them, S1-S represents the 1# cable on the upstream side of Guangzhou direction (small mileage), M7-X represents the 7 # cable on the downstream side of Shanwei direction (large mileage), and G represents the main beam number.

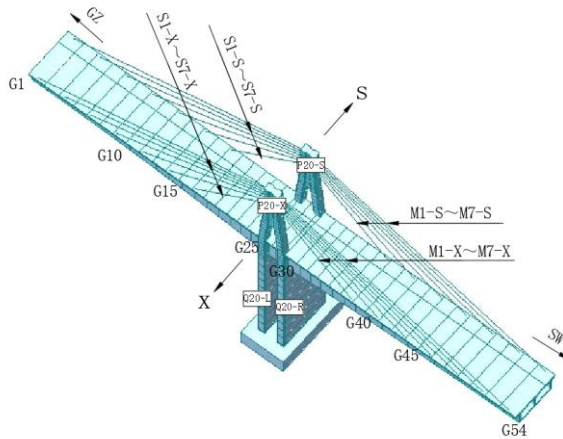


Fig. 2. Finite element model of Boluodongjiang bridge

3 Seismic wave input

Based on the earthquake records provided in the software database, three earthquake records were selected as seismic input, as listed in Table 1; Among them, El - Centro is a regular seismic wave, Chi - Chi is a near field seismic wave, and Mexico is a far field seismic wave. In the table, PGA represents the peak ground acceleration; PGV is the ground peak velocity; G is the acceleration of gravity. The basic seismic peak acceleration of the low tower cable-stayed bridge is 0.3g, and the damping ratio is set to 0.05.

Table 1. Ground motion information

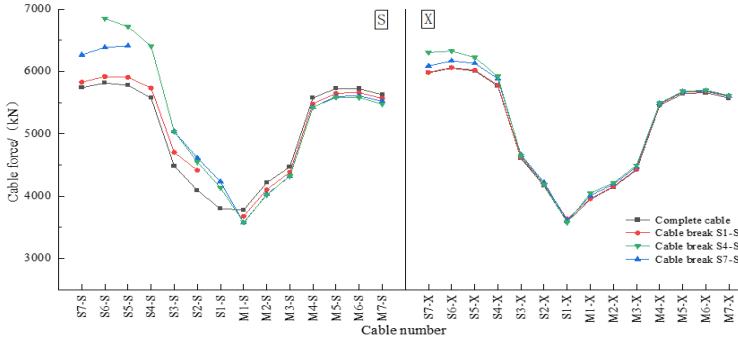
Number	Earthquake	Magnitude	PGA/g	PGV/cm·s ⁻¹
W-1	El-Centro	7.1	0.348	30.9
W-2	Chi-Chi	7.6	0.145	20.8
W-3	Mexico	8.1	0.039	3.3

4 Seismic response analysis

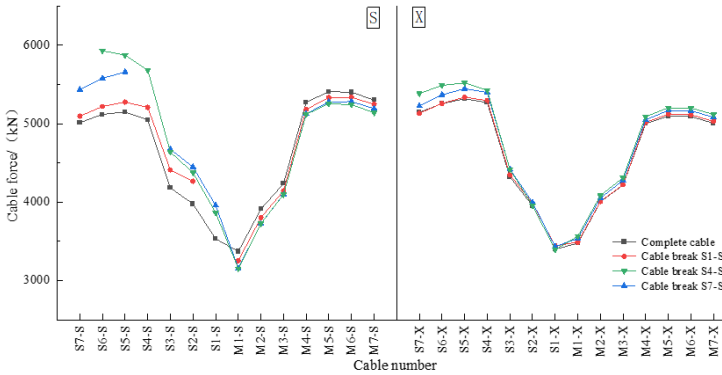
Based on the finite element analysis model, the seismic response of the structure under the condition of broken cables is analyzed, and the variation law of the structure under earthquake action is clarified. The obtained internal force, displacement, and cable force of the structure are combined to accurately evaluate the most unfavorable stress state of the structure under earthquake action.

4.1 Cable

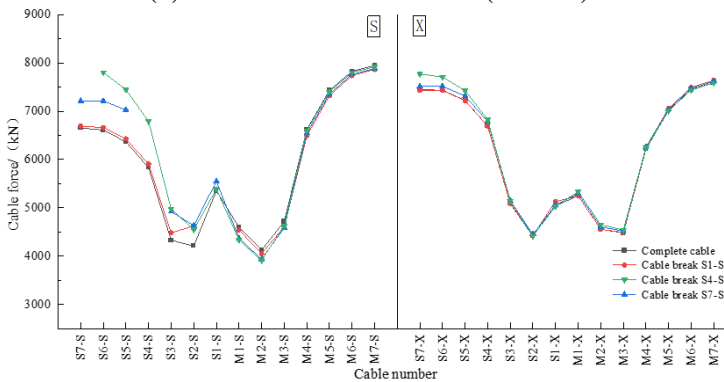
Select the fracture of the upstream side cables (S1-S, S4-S, S7-S) in the Guangzhou direction as a representative, and input three seismic motions along the bridge direction. The maximum cable force curve for each cable is shown in Figure 3.



(a) Peak value of cable tension (El-Centro)



(b) Peak value of cable tension (Chi-Chi)



(c) Peak value of cable tension (Mexico)

Fig. 3. Peak value of cable tension

As shown in Figure 3, under the action of El Centro seismic wave, Chi-Chi seismic wave, and Mexico seismic wave:

(1) The variation of cable force on the upstream side (broken cable side) is relatively obvious, and the variation of cable force on both sides of the cable tower shows an opposite trend. The maximum cable force on the Guangzhou direction cable under broken cable condition is greater than that under unbroken cable condition, and the variation is significant; The maximum and minimum cable forces of the Shanwei directional cable under the broken cable condition are smaller than those under the unbroken cable condition; The variation trend of cable force on the downstream side is smaller than that on the upstream side, and the seismic response under the action of three seismic waves is basically consistent;

(2) The farther the cable break position is from the cable tower, the greater the change in the maximum cable force of the cable; At the same time, the change in cable force adjacent to the broken cable is the largest, showing a decreasing trend in sequence.

The maximum change rate of the cable force under the action of three seismic waves is shown in Table 2. It can be seen that the maximum change rate of the cable force of the stay cable (S1-S) adjacent to the cable tower is between 7.29% and 9.88%, the maximum change rate of the cable force generated by the middle cable (S4-S) fracture is between 12.05% and 13.69%, and the maximum change rate of the cable force when the outermost cable (S7-S) fracture is between 15.85% and 18.08%. From this, it can be seen that the impact of cable breakage on the cable force of the stay cable is between 5% and 20%, which should be taken into account in the corresponding design.

Table 2. Rate of change in cable force of stay cables(%)

Seismic wave	S1-S	S4-S	S7-S
El-Centro	7.87	12.73	17.80
Chi-Chi	7.29	12.05	15.85
Mexico	9.88	13.69	18.08

4.2 Main beam

Three seismic motions were input along the bridge and horizontally to study the influence of cable breakage on the vertical bending moment, torque, and longitudinal displacement of the main beam root of a low tower cable-stayed bridge.

Table 3-5 shows the variation rates of the bending moment and torque at the root of the main beam, as well as the displacement at the beam end, under the action of El Centro seismic waves, Chi-Chi seismic waves, and Mexico seismic waves. It can be inferred that under various seismic actions, the variation rates of the peak vertical bending moment at the root of the main beam are between -3.46% and 7.38%, the variation rates of the peak torque at the root of the main beam are between -0.04% and 4.13%, and the variation rates of the peak longitudinal displacement at the beam end are between -0.22% and 0.32%.

Under the action of El Centro seismic waves, the variation rates of vertical bending moment, torque, and peak longitudinal displacement at the root of the main beam reach their maximum at the S7-7 fracture; Under the action of Chi-Chi seismic waves, the peak vertical bending moment and torque at the root of the main beam change the most during S1-S fracture, and the peak longitudinal displacement at the beam end changes the most during S7-S fracture; Under the action of Mexican seismic waves, the peak values of the vertical bending moment at the root of the main beam and the longitudinal displacement at the end of the beam change the most during the S7-S fracture, and the maximum rate of torque change at the root of the main beam during the S1-S fracture.

When the S1-S cable breaks, the peak vertical bending moment and torque at the root of the main beam have the highest change rate under the action of the Chi-Chi seismic wave, and the peak longitudinal displacement at the beam end has the highest change rate under the action of the Mexico seismic wave; When the S4-S cable breaks, the peak vertical bending moment at the root of the main beam has the highest change rate under the El Centro seismic wave, the peak torque has the highest change rate under the Chi Chi seismic wave, and the peak longitudinal displacement at the end of the beam has the highest change rate under the Mexico seismic wave; When the S7-S cable breaks, the peak values of the vertical bending moment and torque at the root of the main beam have the highest change rate under the action of El Centro seismic waves, and the peak value of the longitudinal displacement at the beam end has the highest change rate under the action of Mexico seismic waves.

Table 3. Peak change rate of El-Centro seismic response(%)

name	S1-S	S4-S	S7-S
M_y	1.29	4.90	7.38
M_z	0.20	1.86	3.15
D_x	-0.04	-0.12	-0.22

Table 4. Peak change rate of Chi-Chi seismic response(%)

name	S1-S	S4-S	S7-S
M_y	3.63	3.73	2.05
M_z	4.13	2.24	0.31
D_x	-0.06	0.02	0.13

Table 5. Peak change rate of Mexico seismic response(%)

name	S1-S	S4-S	S7-S
M_y	-3.46	-0.84	0.17
M_z	1.65	1.03	-0.04
D_x	0.02	0.06	0.32

4.3 Bridge tower

Three seismic motions were input along the bridge and horizontally to study the influence of cable breakage on the top displacement, bottom shear force, and bottom bending moment of low tower cable-stayed bridges. From Table 6-8, it can be seen that under the action of Chi-Chi seismic waves, the time history curves of tower top displacement, pier bottom shear force, and pier bottom bending moment at different locations of cable breakage are basically consistent. The change rate of tower top displacement under cable breakage is between -2.01% and 0.39%, and the change rate of pier bottom shear force and pier bottom bending moment is between -0.04% and 1.05%, and 0.01% and 0.47%.

Under the action of El Centro seismic waves, the peak change rates of tower top displacement, pier bottom shear force, and pier bottom bending moment all reach their maximum at S7-S fracture; Under the action of Chi-Chi seismic waves, the peak shear force and bending moment at the bottom of the main pier change the most at S7-S fracture, while the peak displacement at the top of the tower changes the most at S1-S fracture; Under the action of Mexican seismic waves, the change rates of tower top displacement, pier bottom shear force, and pier bottom bending moment peak all reach their maximum at the S7-S fracture.

When the S1-S cable breaks, the peak displacement of the tower top has the highest rate of change under the action of El Centro seismic waves, the peak shear force at the pier bottom has the highest rate of change under the action of Mexico seismic waves, and the peak bending moment at the pier bottom has the highest rate of change under the action of Chi-Chi seismic waves; When the S4-S and S7-S cables break, the pattern is the same as when the S1-S cables break.

Table 6. Peak change rate of El-Centro pylon seismic response(%)

name	S1-S	S4-S	S7-S
D_x	0.11	0.24	0.39
F_z	0.09	0.42	0.96
M_y	0.01	0.09	0.18

Table 7. Peak change rate of Chi-Chi pylon seismic response(%)

name	S1-S	S4-S	S7-S
D_x	-0.43	-1.20	-2.01
F_z	-0.04	0.04	0.70
M_y	0.08	0.35	0.47

Table 8. Peak change rate of Mexico pylon seismic response(%)

D_x	0.08	0.10	0.13
F_z	0.18	0.53	1.05
M_y	0.02	0.15	0.39

5 Conclusion

Taking the Boluo Dongjiang Bridge as the research object, a finite element analysis model was established using the finite element software Midas Civil2020. In response to the most unfavorable stage of the construction process, the seismic response of the low tower cable-stayed bridge structure under the condition of unilateral cable breakage was analyzed. The main conclusions obtained are as follows:

(1) Under the same seismic wave action, the maximum change rates of beam end displacement, pier bottom shear force, and pier bottom bending moment peak of the structure all occur when the S7-S cable breaks. Under the El Centro and Mexico seismic waves, the maximum change rates of tower top displacement and vertical bending moment peak at the root of the main beam also occur when the S7-S cable breaks; It can be seen that the fracture of the outermost cable has a significant impact on the seismic response of the structure.

(2) When the same cable breaks, the peak change rate of pier bottom shear force and beam end displacement of the structure is the highest under the action of far-field seismic waves (Mexico), the peak change rate of pier bottom bending moment is the highest under the action of near-field seismic waves (Chi Chi), and the peak change rate of tower top displacement is the highest under the action of ordinary seismic waves (El Centro).

(3) Cable breakage only has a relatively significant impact on adjacent cables, and the rate of change in cable force caused by different cable breakage is approximately between 5% and 20%. The impact of cable breakage on the main beam is slightly greater than that of the cable tower. Due to the tower pier beam consolidation system, the overall stiffness is relatively high, so the impact of cable breakage cannot be fully transmitted to the other side of the cable tower, and the impact on the other side is relatively small.

References

1. Li, S.G, Yan, Z.H. (2005) Dynamic performance analysis of partially cable-stayed bridges. *J. Railway Standard Design.*, 02:41-42.
2. Lamesgin, A. Golla, A. (2023) Structural Optimizations of Extradosed Cable-Stayed Bridge by Using Genetic Algorithm. *J. ce/papers.*, 6(5).
3. Wang, K, Xia, X.S, Lu, Z.W., et al. (2022) Effect of cable relaxation on seismic response of single-tower cable-stayed bridges. *J. World Earthquake Engineering.*, 38(03):101-107.
4. Xiang, H.F. (2000) Prospects for World Bridge Engineering in the 21st Century. *J. China Civil Engineering Journal.*, 03:1-6.
5. Chang, B.B. (2008) Research on the Mechanism and Preventive Measures of Cable Damage in Cable-Stayed Bridges. D. Chongqing Jiaotong University., Chongqing.
6. Wei, J.D. (2003) Emergency Repair, Reinforcement and Restoration Project of Xiaonanmen Bridge in Yibin. *J. Highway.*, 04:34-38.
7. Zhang, Y., Fang, Z., Lu, J.B., et al. (2021) Broken cable-induced dynamic response of long-span concrete cable stayed bridge during construction. *J. Journal of Vibration and Shock.*, 40(05):237-246.

8. Mozos, C., Aparicio, A. (2011) Numerical and experimental study on the interaction cable structure during the failure of a stay in a cable stayed bridge. *J. Engineering Structures.*, 33(8).
9. Huang, H., Bai, H., Zhou, W.J., et al. (2021) Dynamic characteristics and seismic performance analysis of V-shaped double steel arch tower cable-stayed bridge with cable damage. *J. Journal of Chang'an University (Natural Science Edition).*, 41(02):114-124.
10. Ali, C., Scott, W., Sherif, M. (2020) Probabilistic Fretting Fatigue Analysis of Bridge Stay Cables at Saddle Supports. *J. Structural Engineering International.*, 30(4):571-579.
11. Xue, X.F., Jin, Q.W., Wang, T.X. (2019) Vulnerability of Long Span Cable-Stayed Bridges in Multiple Damage Scenarios. *J. Journal of Chang'an University (Natural Science Edition).*, 39(05):39-47.
12. Wang, Y. (2023) Research on Dynamic Characteristics and SeismicResponse Study of Extradosed Cable-stayed Bridge Based on Cable Damage. D. Suzhou University of Science and Technology., Suzhou.
13. Xu, X.Y. (2022) Identification and analysis of cable damage in cable-stayed bridges under moving loads based on principal component analysis. *J/Ol. Chinese Journal of Applied Mechanics.*, 1-11.
14. Xiao, Y.G., Lei, Y. (2022) Influence of cable damage on dynamic characteristic of asymmetric single tower cable stayed bridge. *J. Journal of Transport Science and Engineering.*, 38(02):40-44.
15. Xing, X.K., Liu, S., Qin H.Y., et al. (2021) Condition analysis and damage identification for cable damage of cable-stayed bridge. *J. Science Technology and Engineering.*, 21 (5): 2055-2060.
16. Wu, G.R. (2022) Research on Dynamic Responses of the Concrete Self-anchored Suspension Bridge Subjected to the Abrupt Breakage of Hangers. D. Dalian University of Technology., Dalian.

Open Access This chapter is licensed under the terms of the Creative Commons Attribution-NonCommercial 4.0 International License (<http://creativecommons.org/licenses/by-nc/4.0/>), which permits any noncommercial use, sharing, adaptation, distribution and reproduction in any medium or format, as long as you give appropriate credit to the original author(s) and the source, provide a link to the Creative Commons license and indicate if changes were made.

The images or other third party material in this chapter are included in the chapter's Creative Commons license, unless indicated otherwise in a credit line to the material. If material is not included in the chapter's Creative Commons license and your intended use is not permitted by statutory regulation or exceeds the permitted use, you will need to obtain permission directly from the copyright holder.

